GSI 82-41

18 JAN. 1983

GSI

GSI - 82 - 41
PREPRINT

CERN LIBRARIES, GENEVA

CM-P00069055

PREPARATION OF NUCLEAR ACCELERATOR TARGETS BY FOCUSED ION BEAM SPUTTER DEPOSITION

H. Folger, J. Klemm and M. Müller

Dezember 1982

Gesellschaft für Schwerionenforschung mbH
Planckstr. 1 · Postfach 110541 · D-6100 Darmstadt 11 · Germany

Contribution to the 7th CONF. ON THE APPLICATION OF ACCELERATORS IN RESEARCH AND INDUSTRY, Denton, Texas, 8-10 Nov. 1982, to be published by IEEE in Trans. Nucl. Sci. Vol. NS 30, Apr. 1983.

PREPARATION OF NUCLEAR ACCELERATOR TARGETS BY FOCUSED ION BEAM SPUTTER DEPOSITION

H. Folger, J. Klemm, and M. Müller

G S I
Planckstr. 1, 6100 Darmstadt, West Germany

Summary

A duoplasmatron ion source with einzellens extraction was used to prepare focused beams of 10-30 kV of Ar ions with intensities of 1 mA. An em/m-analysis was performed to study the general behaviour of the source. The composition of the beam was investigated to trace and reduce contaminations from extraneous source materials. The Ar-ion beam was applied to sputter milligram-amounts of chemical elements and enriched isotopes of elements having high melting points, such as Zr, Mo, Ru, Ta, W, Ir, etc. The sputtered substances were collected in thicknesses varying from 0.01-2.0 mg/cm^2 onto thin target backings of C, Ti, Cu, or Pb. Self-supported targets were obtained by dissolving backings chemically. Among others, targets of ^{182}W and ^{184}W with thicknesses from 0.19-0.63 mg/cm^2 were thus prepared. Sputtering yields were measured for a series of different target materials. The results are discussed in detail. The targets have been fabricated for various experiments involving high intensity heavy ion bombardments with energies of up to 15 MeV/u of ^{58}Ni, ^{208}Pb, and ^{238}U ions at the GSI UNILAC accelerator.

I. Analysis of the Argon Ion Beam of a Duoplasmatron

The preparation of targets by sputtering strongly depends on the ion-beam quality. The sputtering apparatus of the Sletten-Type[1,2] available from Danfysik, Denmark, does not allow differential beam diagnostics as were the composition of the beam and a detailed control of the ion current. Therefore, the duoplasmatron ion source with extraction system was mounted on an ion-source test bench normally used for PIG source investigations[3].

On this ion-source test bench the source (see Fig. 1) has to be operated at high positive potential as can be seen in an electrical circuit schematics (Fig. 2). The ions are accelerated to ground and transported through a magnetic quadrupole doublet to a 77°5 analyzer magnet. The bending radius of this

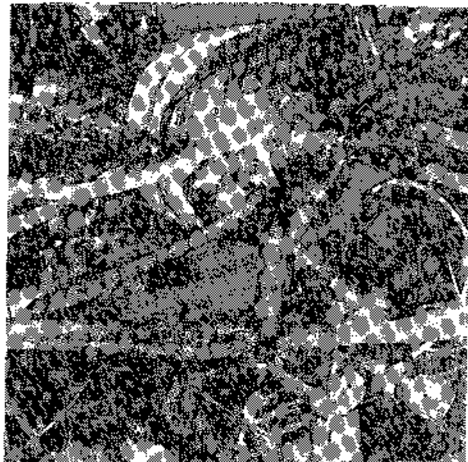

Figure 1. Duoplasmatron (arrow) on an ion-source test bench.

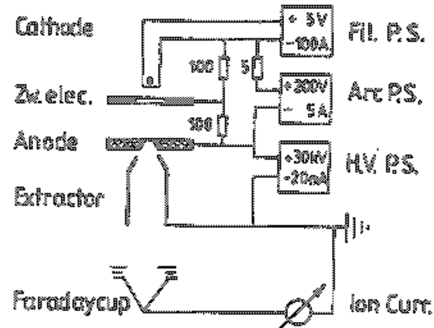

Figure 2. Electrical circuit schematics of the duoplasmatron ion-source for total current measurements.

magnet is 34 cm and the maximum magnetic field strength is 0.7 tesla. A big aperture faraday cup of 30 mm in diameter is placed in the focal point in the deflection plane for e/m-spectra recordings. The whole arrangement can be seen from Fig. 3. Faraday cup 1 is used for measurements of the total extracted ion current versus extraction voltage. As parameters, the arc current, the gas pressure, and the filament current had been varied.

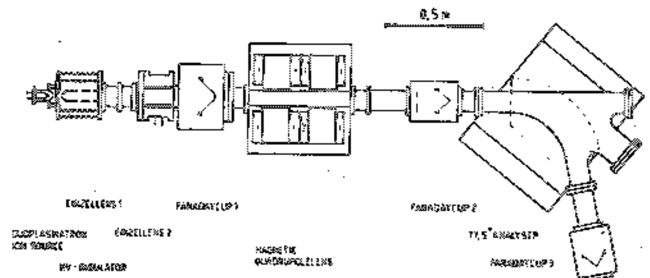

Figure 3. Schematics of the ion-source test bench.

1. Total Current Measurements

a) Variation of arc current (gas pressure 5×10^{-2} mbar; filament current 50 A). — Corresponding to raising arc currents, i.e., raising plasma densities, the extracted ion current available for sputtering of target materials also raises and higher extraction voltages are necessary to reach the plateaus in Fig. 4a. This behaviour is valid between 0.5 and 2.0 A of arc current. Beyond this point the trend is inverting as can be seen from measurements up to 5.0 A in Fig. 4b. A profile through the current/voltage diagrams at 20 kV is given in Fig. 5 to demonstrate this behaviour.

b) Variation of gas pressure (arc current 2 A; filament current 50 A). — The current-voltage function was measured in dependence of the argon gas pressure

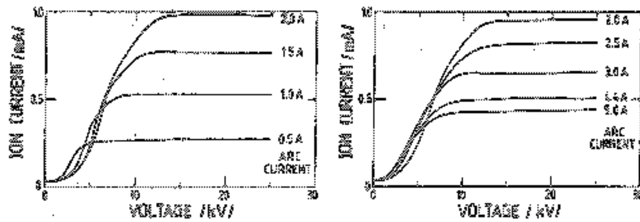

Figure 4. Ion current vs. voltage diagrams for currents of (a) 0.5 to 2.0 A and (b) 2.0 to 5.0 A.

in the source. As shown in Fig. 6, again in a profile of current/voltage curves at 20 kV, the maximum beam intensity is reached at about 5×10^{-2} mbar.

c) Variation of filament current (arc current 2A; gas pressure 5×10^{-5} mbar, diameter of Ta filament 0.8 mm). — Out of another set of current/voltage functions the extracted ion current as a function of the source-filament current was derived (see upper curve in Fig. 7). For this particular case the extracted ion current is constant above 42 A. Higher currents can be obtained below this value, however, the discharge becomes instable, probably due to the rapidly raising arc voltage (see lower curve in Fig. 7).

As a result from the measurements the following optimum conditions for using this ion source in the preparation of nuclear targets by focused ion beam sputtering were derived: The extraction voltage should be higher than 12 kV, an arc current of about 2 A is recommended which can be achieved at an argon gas pressure of 5×10^{-2} mbar, and a filament current of more than 42 A using 0.8 mm diameter tantalum wires.

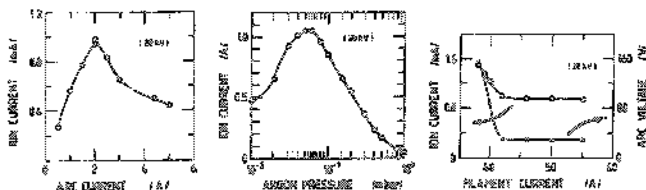

Figure 5. Ion current as a function of arc current (left).

Figure 6. Ion current in dependence of the Ar pressure in the ion source (center).

Figure 7. Ion current (left scale) and arc voltage (right scale) as a function of the filament current of a Ta-wire of 0.8 mm in diameter (right).

2. Mass Analysis

An em/m-analysis by the 77°5 magnet (see Fig. 3) of the ion beam being produced under the outlined condition gives information on the charge states of the sputtergas ions and on the relative amount of contaminations from extraneous source materials.

a) Variation of arc current (gas pressure 5×10^{-2} mbar; filament current 50 A). — The mass spectra show in all cases the dominant Ar^+ peak, illustrated in Fig. 8 for three arc-current values. Log-scale display for the ion current was necessary, as the minor components in the beam were extremely low at low arc currents. As mentioned above (1a) the ion

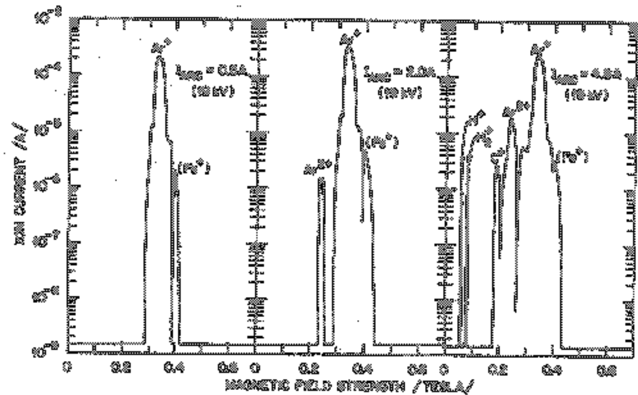

Figure 8. Mass spectra for Ar^+ beams at arc currents of 0.5, 2.0, and 4.8 A.

source should be operated at about 2 A of arc current; at this condition the amount of Ar^{2+} ions is less than 10^{-1}% of the Ar^+ current, and contributions from H_2^+ and C^+ are neglectable. At arc currents of 5A the Ar^{2+}, H_2^+, and C^+ contributions reach intensities of 10% of the Ar^+ current. Differential ion currents of the main components of the beam are plotted versus arc current in Fig. 9.

In the mass range between 50 and 180 AMUs only Fe^+ can be tentatively identified because heavier masses did not appear down to about 10^{-3}% of the Ar^+ intensity. The suppression of iron ions in the beam will be investigated in a separate project with respect to its contribution as contamination in the sputtered target materials.

b) Variation of gas pressure (arc current 2 A; filament current 50 A). — At high gas pressure ($>10^{-1}$ mbar) the ion beam mainly consists out of Ar^+ and Ar^{2+}. Decreasing gas pressure results in the coming up of impurities of H^+, H_2^+, C^+, and masses around Fe^+. This is due to the increasing discharge power which heats up the anode and the zwischen-electrode of the duoplasmatron.

c) Variation of the filament current (arc current 2 A; gas pressure 5×10^{-5} mbar; diameter of Ta filament 0.8 mm). — A similar tendency as found under 2b is observed in the mass spectra (not given

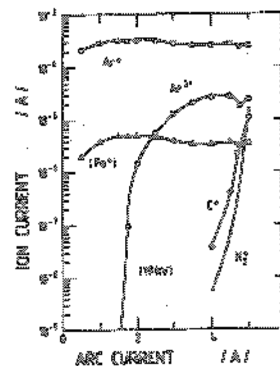

Figure 9. Differential ion currents of the main components of an Ar^+ beam as a function of the arc current.

here) in the course of filament current variation. Electron emission from the cathode is strongly reduced at lower filament currents which is accompanied by arc voltage raise (Fig. 7). At the constant gas pressure the increasing discharge power leads to higher ion beam yield. However, the composition of the beam changes also drastically in the coming-up of impurities, as found similarily already under 2a.

By discussing the data of the mass spectra, optimum source operating conditions were found for the production of a suitably pure Ar^+ beam. These conditions evidently agree with the operating recommendations found during the total current measurements.

II. Focused Ion Beam Sputter Depositions

Ion beams have been used in the investigation of sputtering effects under various aspects. Experimental as well as theoretical treatments of the subject have been given by many authors, as for instance[4,5,6]. The introduction of sputtering into the field of nuclear target preparations was done by G. Sletten and P. Knudsen[1]; they showed that a duoplasmatron ion-source with einzellens extraction can be used to sputter especially effective small amounts of enriched isotopes and high melting-point elements to thin target backings. In addition to sputter depositions with a duoplasmatron[1,2,7,8,9,10] target fabrications were also performed using a penning ion-source[11,12] or a saddle-field ion source[13]. Results from sputter depositions using a duoplasmatron ion-source will be presented here; they will, however, not yet include the experiences gained from the ion-source investigations (see I) made only recently.

1. Sputter Deposition Unit

In a slightly changed sputtering machine of the Sletten-type[1] from Danfysik, Ar-ions are extracted into high vacuum from a duoplasmatron ion-source being equipped with a special gas inlet system maintaining an Ar pressure of $5\cdot10^{-2}$ mbar. The ion beam, having current densities of up to 1.5 mA DC, is focused with an einzellens to a diameter of 1 mm and accelerated with 10 kV to the cathode material; this is sputtered to target backings of C or of Cu, the latter being dissolved after the sputtering to obtain self-supported nuclear targets. Mostly targets of 0.1 to 2.0 mg/cm^2 are fabricated at an area of 15 mm in diameter. The experimental set-up can be seen from Fig. 10. The target backings are mounted on frames being fixed to a rotating target device which can be moved in the X-Y-plane. A view of the rotating target fixture is given in Fig. 11.

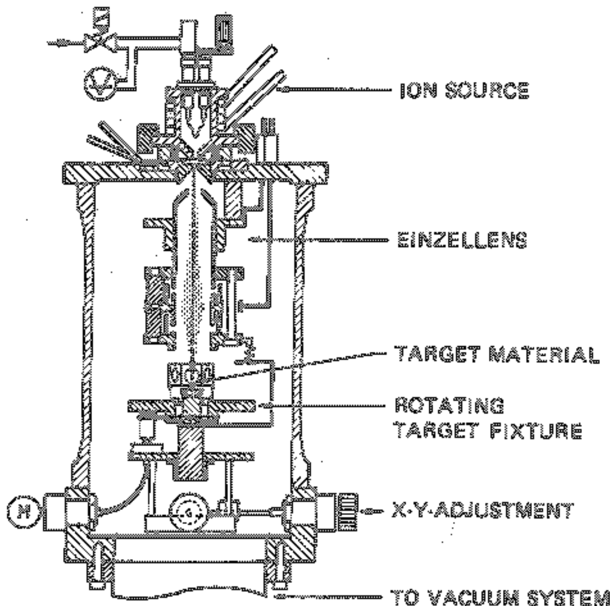

Figure 10. Schematics of the sputtering unit.

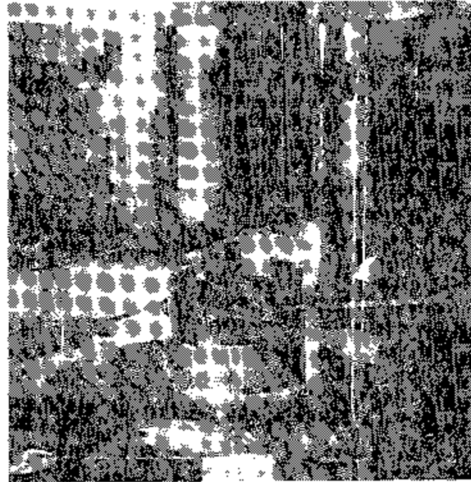

Figure 11. View of the rotating target fixture with special target frames.

2. Deposition Sputtering Yields

Target backings can be arranged around the sputtering cathode at various geometries (see Fig. 10, 11). In order to get a survey on the distribution of target material near the cathode, Ag was collected at constant sputter rates on glass plates mounted at different distances between sputter electrode and target backings. The measured deposition yields in mg/cm^2 are given in Fig. 12 as a function of the distance to the sputtering center. From a comparison - dotted line in Fig. 12 - it can be seen that the distribution nearly follows an expected function of $Y = 1/r^2$ with r being the source-to-substrate distance.

Further measurements of sputter yields were made again with Ag as sputtering material. The deposition

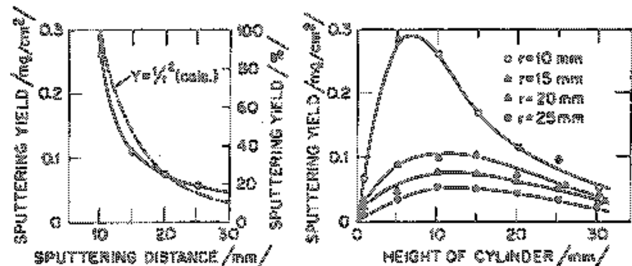

Figure 12. Deposition sputtering yields for Ag as a function of the distance from the cathode material to the target backing (left).

Figure 13. Deposition sputtering yields for Ag at different heights on cylinders of radii of 10, 15, 20, and 25 mm around the cathode (right).

sputter yield was measured as a function of the height on cylinders of radii of 10, 15, 20, and 25 mm around the sputter electrode (Fig. 13). At low geometries (upper curve in Fig. 13) most of the target material is collected with high efficiency at a cylinder height around 5 to 15 mm from the bottom of the rotating target fixture. At larger distances the thickness distribution varies not much at levels from 5 to 25 mm; target backings mounted in this area are quite homogeneous, but the obtained yield per target area is evidently smaller.

Element, Isotope	Cathode-Material mg	Sputtered Material mg	Backing Element mg/cm²	Cathode to Backing Distance mm	Target Yield %/cm²	Target Thickness mg/cm²
^{46}Ti	37.3	1.4	C/0.05	28	4.3	0.06
^{52}Cr	99.9	5.7	C/0.035	36	4.4	0.3
^{54}Cr	43.7	11.3	C/0.030	28	4.4	0.3
^{54}Fe	33.3	9.4	Ta/3.2	42	2.1	0.20
^{58}Ni	49.2	4.0	Au/0.2	42	2.1	0.08
^{60}Ni	26.1	6.1	C/0.030	42	2.3	0.14
^{64}Ni	89.5	16.38	Pb/30	46	2.4	0.39
^{64}Ni	58.4	4.9	Pb/30	40	1.8	0.12
^{92}Zr	171.7	17.3	C/0.036	42	2.6	0.42
^{96}Zr	24.4	2.0	C/0.030	28	4.8	0.13
^{nat}Nb	277.8	3.8	C/0.03	42	2.3	0.1
^{nat}Nb	269.8	2.9	Cu/0.01*	28	3.5	0.10
^{92}Mo	153.1	5.2	C/0.025	42	2.3	0.11
^{94}Mo	73.2	3.95	C/0.04	28	4.0	0.18
^{96}Mo	64.0	4.5	C/0.04	28	1.9	0.19
^{100}Mo	137.4	3.4	C/0.033	28	4.1	0.14
^{100}Mo	143.2	3.9	C/0.030	42	1.7	0.1
^{96}Ru	28.4	2.8	C/0.035	28	4.6	0.13
^{98}Ru	60.4	9.3	C/0.090	25	5.2	0.38
^{98}Ru	48.3	8.1	C/0.065	25	4.9	0.40
^{99}Ru	169.6	9.3	C/0.035	42	1.7	0.16
^{99}Ru	101.5	4.8	C/0.025	28	3.9	0.19
^{100}Ru	130.2	6.7	C/0.03	42	1.7	0.15
^{102}Ru	93.3	20.5	C/0.035	42	2.3	0.48
^{104}Ru	66.5	20.5	C/0.034	42	2.0	0.5
^{104}Ru	78.3	42.6	^{208}Pb/50	25	4.7	2.0
$^{nat}Nd_2O_3$	35.0	15.5	C/0.035	28	2.7	0.42
$^{148}Nd_2O_3$	39.0	14.8	C/0.030	28	3.7	0.55
$^{146}Nd_2O_3$	36.5	16.2	C/0.030	28	3.8	0.61
$^{150}Nd_2O_3$	35.0	18.6	C/0.035	28	3.0	0.55
^{nat}Ta	977.5	8.08	Cu/0.01*	28	3.9	0.27
^{nat}Ta	986.0	5.32	Cu/0.01*	28	4.0	0.25
^{nat}Ta	262.6	11.0	C/0.025	40	1.7	0.19
^{nat}Ta	237.2	15.7	C/0.030	40	2.1	0.34
^{nat}Ta	585.6	4.3	Cu/0.01*	42	2.0	0.09
^{180}W	7.8	7.7	Al/1.35	25	3.6	0.28
^{182}W	138.2	8.4	C/0.037	28	3.6	0.3
^{183}W	121.8	6.22	C/0.035	28	4.3	0.28
^{182}W	75.9	11.56	Cu/0.01*	28	3.5	0.41
^{184}W	41.2	5.80	C/0.035	28	4.3	0.23
^{184}W	58.3	21.10	Cu/0.01*	28	3.1	0.65
^{184}W	53.2	8.15	Cu/0.01*	28	3.5	0.28
^{184}W	36.5	6.0	C/0.040	26	3.2	0.2
^{184}W	914.1	51.1	C/0.03	42	1.0	0.55
^{184}W	72.5	36.0	^{208}Pb/50	26	3.7	1.4
^{186}W	210.0	9.6	C/0.034	25	4.2	0.4
^{nat}Re	237.7	27.4	C/0.03	42	1.1	0.3
^{191}Ir	176.4	29.3	Ti/0.95	25	4.8	1.0
^{193}Ir	286.0	78.6	Cu/9.0	30	3.2	2.5
^{nat}Ir	1547.0	2.7	Cu/0.01*	28	3.7	0.10
^{nat}Pt	198.9	8.0	C/C5	56	0.9	0.07

nat = natural occurring element
* = intermediate Cu backing (0.01 mm thick) in the preparation of self-supported targets

Tab. 1. Compilation of data from target preparations by sputter depositions with a focused ion beam of 10 kV of Ar^+ at 0.5 to 1.3 mA.

3. Sputter Deposition of Accelerator Targets

The focused ion-beam sputtering process was used in the preparation of many accelerator targets. It was of interest in all cases where only small amounts of target materials, especially of enriched stable isotopes, were available. The procedure was also very efficient in the preparation of target foils from high melting-point elements. For the following elements and for some oxides experience in the preparation of nuclear targets was gained over the last years: Ag, Al, Au, Cr, Fe, Ge, Hf, HfO_2, Ho, Ir, Mn, Mo, Nb, Ni, Os, Pd, Pt, Re, Rh, Ru, Sn, SrO, Ta, Ti, W, and Zr. A compilation of data from about 50 different target preparations is given in Tab. 1. The elements or enriched isotopes being used as sputtering materials are listed in the first column of the table arranged after increasing atomic numbers. The available amount of cathode material varied: it was 7.8 mg for ^{180}W, 50 to 200 mg for most of the materials listed, and - at random - 1547 mg for Ir. The amount of cathode material being sputtered off the cathode was depending on the needs for the target thickness in question and it varied between 1.4 mg (^{46}Ti) and 78 mg (^{193}Ir). The target backings most often needed were foils of carbon of about 0.03 mg/cm²; among others copper foils of about 0.01 mm were taken as backings being dissolved after the sputter depositions in order to obtain self-supported targets (see Tab. 1, col. 4). The cathode-to-backing distance was 28 to 56 mm, depending on the amount of targets to be made in one run and on the desired thickness of the target layer. The target yield is related to the amount of sputtered materials and to the thickness of the target; it is given in percent per square centimeter. This figure strongly depends on the geometrical set-up in the sputter apparatus; of great influence are also the sputtering yields (number of sputtered atoms per incident ion, mostly having values between 1 and 50) and the form of crystallographic structures of the surfaces of the sputter cathode. The knowledge of these figures in a sputter system is of importance for further target preparations. The last column of Tab. 1 contains the target thicknesses which were obtained in the preparations; the area densities of the produced layers vary between 0.07 mg/cm² (Pt) and 2.5 mg/cm² (^{193}Ir). A picture of five targets is given in Fig. 14.

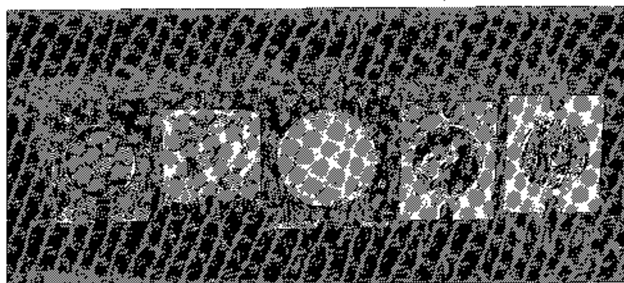

Figure 14. Sputtered nuclear targets of ^{96}Ru, ^{98}Mo, ^{104}Ru, and Ta on carbon backings and self-supported ^{184}W foil (left to right).

4. Applications of the Sputtered Targets

The targets which were prepared using an Ar^+ beam in a focused ion-beam sputtering apparatus were used in heavy-ion accelerator experiments at the GSI UNILAC in Darmstadt. Nuclear physics, atomic physics, and nuclear chemistry reaction studies were performed

using accelerator beams of high energies of up to 15 MeV/u of ^{58}Ni, ^{208}Pb, or ^{238}U with intensities of up to $5 \cdot 10^{12}$ particles per second.

III. Concluding Remarks

The analysis of the beam of a duoplasmatron ion-source on an ion-source test bench gives important information which can be used to optimize the intensity and the quality of an extracted beam to be applied in sputter depositions in target preparations.

With the apparatus being applied to focused ion-beam sputter depositions, many targets can be prepared of small amounts of enriched isotopes and of high melting-point elements which could not or only very difficult be prepared by other target preparation procedures.

References

1. G. Sletten and P. Knudsen, Nucl. Instr. and Meth. 102, 459 (1972).

2. G. Sletten, Proc. Annual Conf. of the International Nuclear Target Development Society, Chalk River, Ontario, 1974 (AECL-5503) p. 52.

3. M. Müller, this conference.

4. R. Behrisch, Ergebnisse der exakten Naturwissenschaften 35, 295 (1964).

5. P. Sigmund, Phys. Rev. 184, 383 (1969).

6. P. D. Townsend, J. C. Kelly and N. E. W. Hartley, Ion Implantation, Sputtering and their Applications (Academic Press, London 1976), p. 111 ff.

7. W. A. Scaife, P. R. Hanley and K. H. Purser, Proc. 4th Annual Conf. of the International Nuclear Target Development Society, Argonne National Laboratory, Argonne, Illinois, 1975 (ANL/PHY/MSD-76-1) p. 75.

8. J. K. Kwinta, Nucl. Instr. and Meth. 167, 65 (1979).

9. G. Sletten, Nucl. Instr. and Meth. 200, 21 (1982).

10. J. Kwinta and J. J. Michel, Proc. 11th Annual Conf. of the International Nuclear Target Development Society, Seattle, Washington, 1982 (to be published).

11. H. Baumann and H. L. Wirth, Proc. 6th Annual Conf. of the International Nuclear Target Development Society, Berkeley, California, 1977 (LBL-7950) p. 121.

12. H. Baumann and H. L. Wirth, Nucl. Instr. and Meth. 167, 70 (1979).

13. R. J. Drinkwater, Proc. 11th Annual Conf. of the International Nuclear Target Development Society, Seattle, Washington, 1982 (to be published).